Draft version July 27, 2019
Typeset using LaTeX **modern** style in AASTeX62

Testing and Iterating upon the AIRFLOW turbulence sensor

Jacob Young[1] and Mark Chun[2]

[1] *San Jose State University*
1 Washington Square, San Jose, CA 95195, USA
[2] *University of Hawaii Institute for Astronomy*
640 N Aohoku Pl, Hilo, HI 96720, USA

1. ABSTRACT

AIRFLOW is a device which measures local optical turbulence by analyzing interference patterns created by a non-redundant pinhole mask. We can use AIRFLOW to determine where optical turbulence is most prevalent within the telescope domes. Here, we determine how the instrument will be operated and we quantify the limitations of its measurements. We also test various design iterations which include a new pinhole mask, a removable instrument cover and code which autonomously runs the instrument and processes data received. Baseline tests indicate the instrument's measurement floor of C_n^2 to be two orders of magnitude lower than the mean value seen at previous tests in turbulent environments. In this paper we present the details of the design iterations as well as the procedure for tests that prove the data validity of the instrument.

2. INTRODUCTION

When in an atmosphere, image quality is degraded by optical turbulence present in the air. The more optical turbulence, the lower the given image quality (Nash 2014). This optical turbulence can roughly be separated into three given layers: the free atmosphere, where turbulence occurs at the upper edge of the troposphere boundary layer; the ground layer turbulence which occurs due to the interaction between the wind and the local landscape as well as other obstacles such as telescope domes; and the turbulence present within the observatory dome itself(Chun et al. 2009). Turbulence in the free atmosphere behaves mostly according to Kolmogorov statistics with a larger outer scale (L=10-100m) (Lai et al. 2019) causing low frequency aberrations. Closer to the ground, the turbulence has a much smaller upper scale the order of the size of telescope domes. Within the dome, the upper scale of the turbulence drops, creating higher frequency optical turbulence. From

Corresponding author: Jacob Young
jacob.daniel.young@gmail.com

wavefront sensor data, we expect dome seeing within the University of Hawaii 2.2 meter telescope. The specific location of the turbulence within the dome is still unknown, but it accounts for nearly 1/3 of the turbulence the light encounters before entering the pupil(Chun et al. 2009). To mitigate this in-dome turbulence, we must first find its exact source. Possibilities include the air around the structure of the dome itself, the air in the tube, or the air directly above the mirror(Lai et al. 2019).

2.1. *Theory*

Optical turbulence occurs when two mediums with different indices of refraction mix. In the case of optical turbulence in the atmosphere, it occurs when pockets of air with different temperature mix. When a planar wavefront enters the atmosphere, these mixing pockets cause the refractive index of the air to vary spatially which introduces aberrations in the wavefront. This variance can be quantified in the spatial domain by the structure function:

$$D_n(\rho) = \langle |n(r) - n(r+p|^2 \rangle. \tag{1}$$

In this equation, $n(r)$ is value of the refractive index at a point r and at another point $r+p$ (Nash. 2014). By assuming that the air is both homogeneous and isotropic, the structure function can be represented as

$$D_n(\rho) = C_n^2 \rho^{2/3}, \tag{2}$$

where term C_n^2 describes the index structure constant and represents the energy of the local optical turbulence.

3. METHODOLOGY

3.1. *Methods*

Lai et al. 2019 introduce an approach to directly measure the optical turbulence using a non-redundant mask imaging interferometer. This device, AIRFLOW, measures the variation in the interference pattern created by a set of pinholes to infer the optical path difference between pinhole pairs. From these optical path differences, we can infer the the Phase Structure Function D_ϕ (Lai et al. 2019). This Phase Structure function is then fit with a model to find the Fried Parameter r_0 .This parameter roughly represents the effective diameter of a telescope as it equates the diffraction limit to the seeing. Formally, it is the diameter of a region which has a phase variance of 1 rad^2. The quantity r_0 can also be written as an integral of the index structure constant C_n^2 along a given distance, in this case the length of the instrument's sampling area

$$r_0 = \left[0.423k^2 \int_0^L C_n^2(h)dh\right]^{-3/5}. \tag{3}$$

In this equation, k is the wave number equal to $2*\pi/\lambda$ and L is the sampling distance. This equation can be simplified into equation 4 by assuming C_n^2 is constant within the sampling area(Lai et al. 2019)

$$r_0 = 1.68(k^2 C_n^2 L)^{-\frac{3}{5}}. \tag{4}$$

By obtaining r_0 from the Phase Structure Function fit, and determining k and L from the instrument, C_n^2 can be calculated using eqaution 4.

By placing AIRFLOW in various positions around the observatory (scaffolding, outside the mouth of the tube, inside the tube, directly above the mirror, etc) we can determine where the C_n^2 value is highest throughout multiple day-night temperature cycles.

3.2. *Instrument Design*

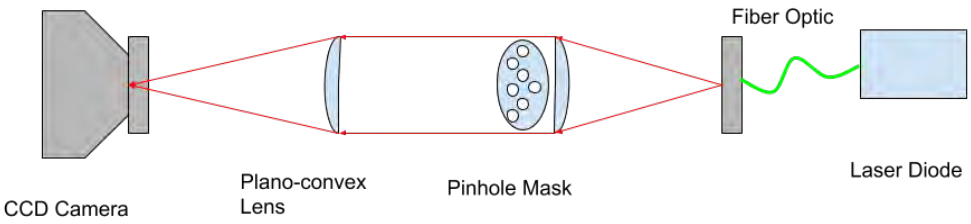

Figure 1. Simplified diagram of AIRFLOW

To create an interference pattern that can be interpreted, AIRFLOW uses two assembled sections. The first section is comprised of a 5mW, 635 nm laser which is directed into the system using a single mode fiber optic cable. The diverging beam is placed at the focal length of a plano-convex lens, collimating it as it enters the sampling area as shown in figure 1. The non-redundant pinhole mask is placed directly after the first plano-convex lens and creates the interference pattern which is distorted by optical turbulence in the sampling area. The now perturbed interference pattern is focused by a second plano-convex lens into a CCD camera placed at the latter lens' back focal plane. Images are taken with exposures measured in the μs range, and are interpreted by code which measures the difference in each image due to the optical turbulence present in the sampling area. The interference pattern created by the pinhole mask can be seen in figure 2.

The instrument is assembled from COTS (Consumer Off The Shelf) components that are assembled on a dovetail rail. This way, the entire system is fully modular and components can be replaced and moved with general ease. Due to its modular nature, the instrument can also be assembled with relatively little mechanical or technical skill.

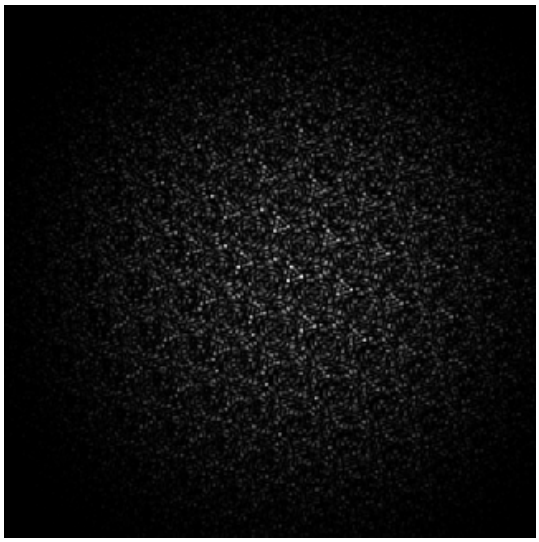

Figure 2. Interference pattern created by an 18-hole non-redundant pinhole mask

3.3. *Pinhole Mask*

The non-redundant pinhole mask is a vital component of the AIRFLOW instrument as it is responsible for the interference pattern that allows turbulence to be measured. Initially the pinhole mask used was 3D printed from PLA. It was predicted that a pinhole to diameter ratio of 1:100 was optimal for a mask approximately 24mm in diameter. However, due to the imprecision of the 3D printer, a ratio of only ≈1:24 with 1mm holes was achieved for the first iteration of the pinhole mask as shown in figure 3.

To achieve the 1:100 ratio, a new design was drafted with the intent of being laser cut from stainless steel as shown by figure 4. This manufacturing process allows for a precision much higher than that of 3D printing and enabled the desired pinhole mask to be made. The current pinhole mask was made using this technique and produced an interference pattern double the size of the previous pinhole mask.

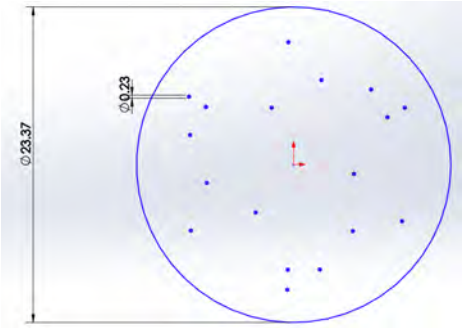

Figure 3. CAD drawing of the laser cut mask with 0.23mm holes 1/100th the diameter of the mask

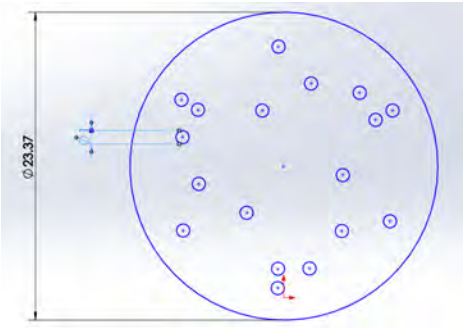

Figure 4. CAD drawing of the 3D printed mask with 1mm holes 1/24th the diameter of the mask

3.4. *AIRFLOW Covers*

Much of AIRFLOW's functionality depends on isolating dim points of light from a dark background. The larger the contrast between background noise and the points, the larger the SNR(Signal-to-Noise-Ratio) and data precision. Moreover, as the equations used to calculate the turbulence from the OPD relies on optical turbulence only occurring within the sampling area, any optical turbulence that interferes with the light outside of this area will skew the data. To ensure that as little environmental light and external optical turbulence enters the system outside of the sampling area, the open space between the camera and its lens, and the laser and its lens should be covered. The first iteration of these covers were made from a thin sheet of flexible nitrile rubber. Though easy to attach and remove, these covers still allowed in light from direct sources and were poor insulators, allowing optical turbulence to develop in the areas outside of the sampling area. To counteract these issues, rigid covers 3D printed from black PLA plastic were designed and manufactured as shown in figure 5. These PLA covers are sturdier and far more robust that the nitrile covers, increasing the resilience of the instrument from adverse environments as well as its accuracy.

Figure 5. AIRFLOW 3 fully assembled

4. RESULTS AND DISCUSSION

Instrumentation design comes hand in hand with rigorous testing to ensure the validity of any data retrieved by the instrument itself. The first step of this process is to establish the noise floor of the instrument. This allows actual data to be distinguished from noise inherent to the system and establishes the lowest measurement the instrument is capable of making.

4.1. *Instrument Baseline*

AIRFLOW is first placed into a controlled environment which minimizes sample contamination due to external turbulence and temperature difference. This is achieved

by placing AIRFLOW in an area exposed to as few radiative heat sources as possible, and away from regularly moving air. During the control test on 07/19/19, this was done by placing AIRFLOW under a desk in a small temperature controlled room, wrapping the center sampling area with rubber, enclosing the sampling area in a Styrofoam box, and covering the entire apparatus with a cardboard box. It is important to note that camera is a significant source of both moving air and radiative heat, so should be blocked off from the rest of the apparatus as shown in Figure 6.

Figure 6. Images of the control experiment setup AIRFLOW covered by a carboard box over the Styrofoam box (left) AIRFLOW's sampling area covered in a Styrofoam box (right)

Once isolated from external heat, light, and moving air, a data collection program which takes a set amount of captures every 5 minutes is executed. This program isolates the interference pattern in a 456×456 pixel square and runs it through data reduction code. Camera options are set to ensure the image contains no saturated pixels and attains the highest SNR possible as shown in table 1. Data is collected in sets comprised of several captures of at least 100 FITS images. If a capture fails, a replacement capture is taken.

Starting in the evening of 07/19/19, two sets of 4 captures each comprised of 500 FITS were taken once every five minutes for 24 hours. The mean of every 4 points of data was taken to be plotted as seen in figure 7. A python script then took the mean and standard deviation(STD) of all 1728 points of data detailing the minimum and maximum C_n^2. These results are listed in table 2.

Bin	Image Format	Gain	Exposure (μs)	Brightness	Bandwidth	Laser Power
1x1	16bit	0	75	0	100	High

Table 1. Camera Settings

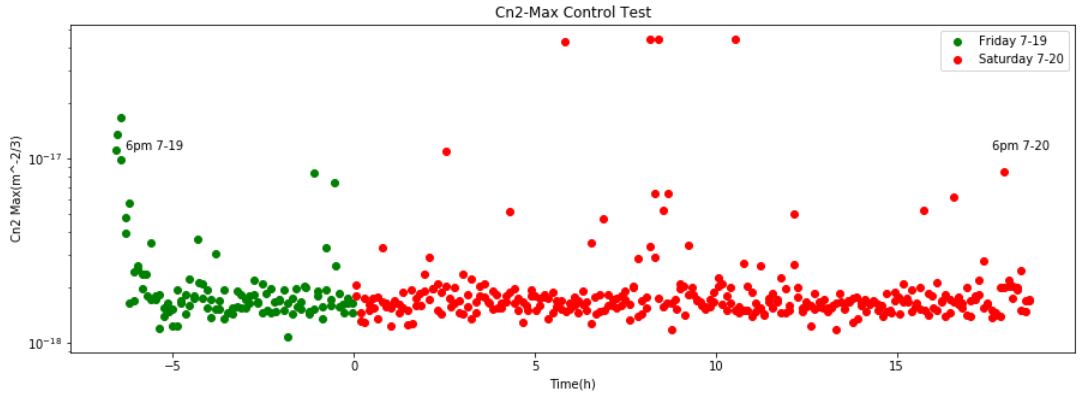

Figure 7. Control test taken for ≈ 24 hours from 7/19/19 until 7/20/19 to determine the AIRFLOW"s noise floor of C_n^2 values

STD of C_n^2 min	STD of C_n^2 max	Mean of C_n^2 min	Mean of C_n^2 max
8.85×10^{-19}	8.76×10^{-18}	1.11×10^{-18}	2.40×10^{-18}

Table 2. Baseline test results

This set of data determines the noise floor for all measurements taken by AIRFLOW. Any data measured below this point or within its standard deviation can be attributed to instrument error and ignored.

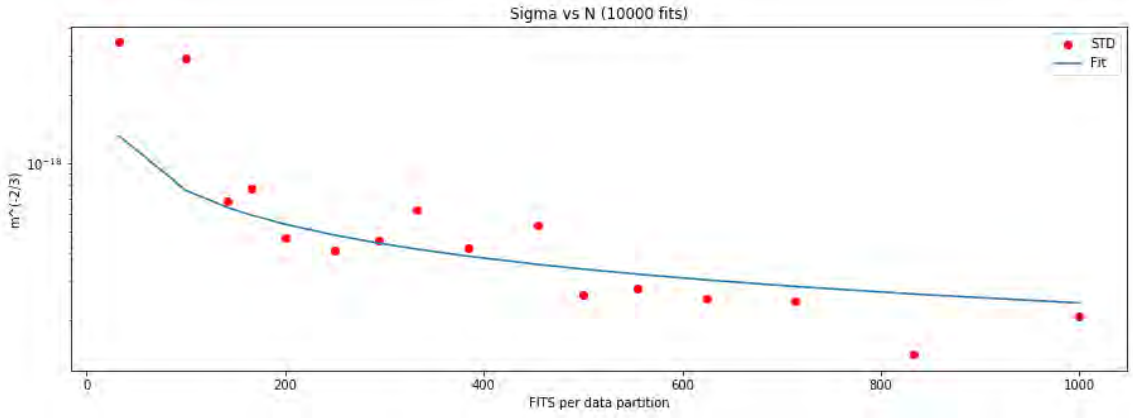

Figure 8. Standard Deviation of C_n^2 max values reduced from different sized partitions

A second test was was performed to determine if the system contained any error other than the Standard Error of $1/\sqrt{N}$. In the test, a very large dataset, comprised of 10,000 FITS, was split into partitions and reduced by the AIRFLOW code, providing a maximum C_n^2 value for each partition. Each partition was comprised of every nth

FITS file in the dataset, where n is the number of partitions. This was done to limit any time-borne variation in the data. Partition sizes ranged from 10 sets of 1000 FITS to 300 sets of 33 FITS. The standard deviation of the C_n^2 values for each set of partitions taken and plotted as shown in figure 8. As the amount of FITS in a given partition increases, the standard deviation decreases. The plot seems to follow the trend of standard error in a statistical system, leading us to believe any mechanical error can be neglected in the statistical error's presence. This plot can also show us the optimal dataset size to be taken during actual experiments. The standard deviation begins to flatten out after a set size of 500, leading us to believe that the best sample size is in the range of 500-700 FITS per set. This assertion can be made because the decrease in data processing time of the AIRFLOW code for samples sized below 700 outweighs the benefit of a minor increase in precision for sample sizes over 700.

4.2. *Future Plans*

In future tests, the device could be placed in a more thermally constant area, and several days worth of data could be taken. We predict the mean values of C_n^2 would further decrease as a result of this. However, in previous AIRFLOW tests performed at the Canada France Hawaii Telescope as shown in figure 9, maximum C_n^2 values measured did not go below $10^{-16}\mathrm{m}^{-2/3}$, two orders of magnitude above AIRFLOW's noise floor, making the currently noise floor adequate for any future tests performed in an observatory setting.

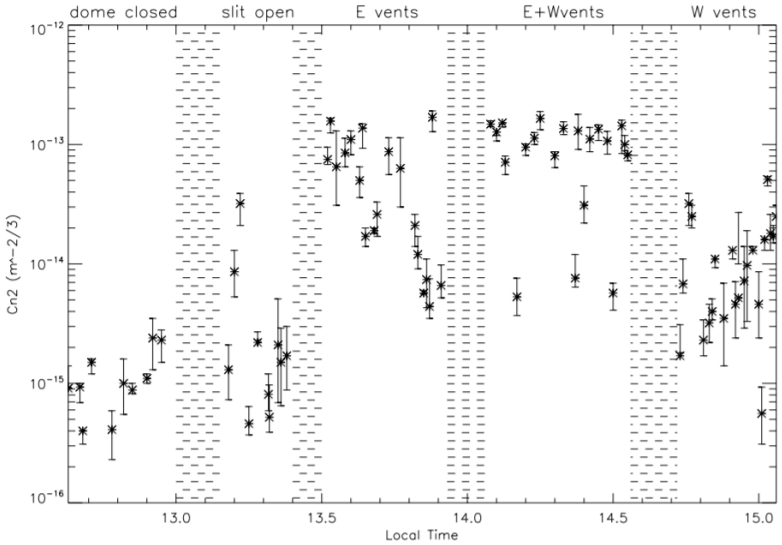

Figure 9. Graphed C_n^2 values from tests performed at CFHT (Lai et al. 2019)

To properly determine the location of the optical turbulence within the observatory, more steps still have to be taken. Several AIRFLOW instruments should be placed around the dome, collecting data continuously for several years. The turbulence measurements from AIRFLOW should be combined with a suite of other environmental data including temperature, wind speed, and wind direction with respect to the slit. By combining all of these datasets, we hope to create models of the observatory turbulence based on different environmental conditions. Once there is enough data to establish trends of optical turbulence based upon environmental conditions, we can begin to determine where it is most prevalent.

5. CONCLUSION

We developed a new instrument that directly measures local optical turbulence to create a model of the optical turbulence within an observatory. To perform tests with this instrument, it first had to be calibrated and tested to establish measurement accuracy and a noise floor. The instrument's design was iterated upon with end goal to further increase data quality. These steps included designing a new pinhole mask with more precise pinholes which contributed to a higher level of data accuracy and designing rigid covers to keep several components on the instrument in a controlled, isolated environment. The latter will reduce environmental noise. Control experiments indicated AIRFLOW's noise floor to be two orders of magnitude lower than the weakest optical turbulence experienced in the previous experiments at CFHT. This leads us to believe that all data gathered at the UH88 telescope site will be usable as none will be below or within the error of AIRFLOW's noise floor.

REFERENCES

[1]Chun, M. , Wilson, R. , Avila, R. , Butterley, T. , Aviles, J. , Wier, D. and Benigni, S. (2009), Mauna Kea groundlayer characterization campaign. Monthly Notices of the Royal Astronomical Society, 394: 1121-1130.

[2]Lai, O., Withington, J. K., Laugier, R., Chun,M., 2019, Direct measure of dome seeing with a localized optical turbulence sensor

[3]Nash. R., 2014, Design and Implementation of the Tip/Tilt Compensation System for Raven, a Multi- Object Adaptive Optics System, (MAS), University of Victoria.